Double Slit

October 09, 2016

Author: Jacob Cluff

Partners: Josef Rinderer, David Turk

Abstract:
In this experiment, Compton scattering is explored. A Multi-Channel Analyser (MCA) is used to collect photons scattered off the target. The electron rest energy is found to be 468.96 with a 8.2271% error from the known value and uncertainty of 105.80 keV. The differential cross sections for scattering angles [20, 30, 40, 50, 60, 70, 80, and 90] are found to be [20.337, 15.395, 13.118, 7.6978, 2.4332, 4.8284, 8.3417, 5.5829] $\times 10^{-27} cm^2 \pm$ [8.836, 6.689, 5.700, 3.345, 1.058, 2.098, 3.625, and 1.992] $\times 10^{-27} cm^2$. The average uncertainty in the differential cross section is 4.168 $\times 10^{-27} cm^2$.

Introduction:

When an atom in a radioactive source decays, it emits a high energy photon. In this experiment, the source is put into a lead casing that allows only a narrow beam through, which is aimed at an aluminum target. When the high energy photon hits an electron in the target, it gives a portion of its energy to the electron, which is enough for it to break away with a large recoil energy. With extremely large photon energies, the electron can often be treated as a free electron, rather than being bound to an Al atom in the target.

When this scattered electron hits the NaI crystal, it quickly decelerates. The resulting bremsstrahlung radiation causes a quick flash of light, or scintillation, which is picked up by a Photo-Multiplier Tube (PMT). The PMT converts this flash of light into an electrical pulse that is measured by the instruments.

Theory:

Equation 1 below describes how the photon's wavelength will lengthen after scattering off a "free" electron. After it deposits energy to the electron, it has lower energy; from the energy wavelength relationship ($E_\gamma = \frac{hc}{\lambda}$), it is readily seen why the scattered photon will have a longer wavelength. This shift in energy is proportional to the Compton wavelength and a relation with the scattering angle that preserves conservation of energy and momentum. In the form presented at the end of Equation 1, it can be seen that a plot of the inverse scattering energy, as a function of $(1 - \cos\theta)$, should result in a straight line. The slope of this line should be the inverse of the electron's rest mass and the y-intercept should be the inverse energy of the incident photon's energy.

$$\begin{aligned} \Delta\lambda = \lambda_s - \lambda_o &= \lambda_C(1 - \cos\theta) \\ E = \frac{hc}{\lambda} &\Rightarrow \lambda = \frac{hc}{E} \\ \Rightarrow \frac{hc}{E_s} - \frac{hc}{E} &= \frac{h}{mc}(1 - \cos\theta) \\ \Rightarrow \frac{1}{E_s} &= \frac{1}{mc^2}(1 - \cos\theta) + \frac{1}{E} \end{aligned} \tag{1}$$

where λ_s and E_s are the scattered wavelengths and energies, λ and E are the un-scattered wavelengths and energies, and θ is the scattering angle.

Equation 2 gives the differential cross section, where $d\Omega$ is the solid angle of the detector seen from the target, N_e is the number of illuminated electrons in the target, and σ is the cross section itself. The pieces needed to calculate the differential cross section are constructed in Equations 3 through 8.

$$\frac{d\sigma(\theta,\varphi)}{d\Omega} = \frac{\left(\frac{\#scattered/s}{d\Omega}\right)}{N_e\left(\frac{\#inc/s}{A}\right)} \tag{2}$$

$$\begin{aligned} R(R_0, t_c) &= \text{Decay rate of } {}^{137}Cs \\ &= R_0 e^{t_c/43.28\ yrs} \\ R_0 &= \text{decay rate at calibration time}, t_c \\ \Rightarrow R(\ 5.46\ mCi = 2.0202e8\ decays/sec\ ,\ 21.5\ yr\ ) &= 1.2293 \times 10^8\ decays/sec \end{aligned} \tag{3}$$

$$\begin{aligned} A(r_{ts}) &= \text{Area of sphere at distance from source to target, } r_{ts} \\ &= 4\pi r_{ts}^2 \\ \Rightarrow A(15.24\ cm) &= 2.9186 \times 10^3\ cm^2 \end{aligned} \tag{4}$$

$$
\begin{aligned}
I_{inc} &= \text{Incident intensity} \\
&= \frac{R(R_0, t_c)}{A(rts)} \\
\Rightarrow I_{inc} &= \frac{1.2293\times^{8}}{2.9186 \times 10^3}\ decays/s/cm^2 \\
&= 42118\ decays/s/cm^2
\end{aligned}
\tag{5}
$$

$$
\begin{aligned}
N_e &= \text{Number of electrons in target} \\
&= (\#\text{ atoms})(\#\text{ electrons/atom}) \\
&= (\text{volume of target})(\text{density of target})(\#\text{ atoms/mass})(\#\text{ electrons/atom}) \\
&= (\pi r_t^2 h_t)(\rho_{Al})(\text{mols/grams}_{Al})(\text{Avogadro's number})(n_{e,Al}) \\
&= (\pi 15.24^3 cm^2 h_t)(2.7\ g/cm^3)(3.7062e-2\ mols/grams)(6.022e23\ mol^{-1})(13\ electrons/Al\ atom) \\
&= 2.2913 \times 10^{24}\ electrons
\end{aligned}
\tag{6}
$$

$$
\begin{aligned}
d\Omega &= \text{solid angle of detector seen from target} \\
&= \frac{\text{area of detector}}{\text{target to detector distance}^2} \\
&= \frac{\pi d_{detector}^2}{4}\frac{1}{r_{dt}^2} \\
&= \frac{\pi\ 4.445^2 cm^2}{4}\frac{1}{35.56^2 cm^2} \\
&= .012272\ sr
\end{aligned}
\tag{7}
$$

$$
\begin{aligned}
\frac{d\sigma}{d\Omega} &= \frac{\text{yield}}{d_\Omega N_e I_{inc}} \\
&= \frac{\text{yield}}{(.012272\ sr)(2.2913 \times 10^2 4\ electrons)(42118\ decays/s/cm^2)} \\
&= \frac{\text{yield}}{1.1843 \times 10^{27}}\ cm^2
\end{aligned}
\tag{8}
$$

$$
\begin{aligned}
\text{yield} &= \text{sum of all counts recorded by MCA} \\
\text{corrected yield} &= \text{yield}\frac{\text{peak to total ratio}}{\text{quantum efficiency}}
\end{aligned}
\tag{9}
$$

The corrected yield found in Equation 9 is used in calculating the differential cross section in Equation 8. The peak to total ratio and the quantum efficiency are taken from Table 3. Corroborating graphs are found below (Figures 1 and 2).

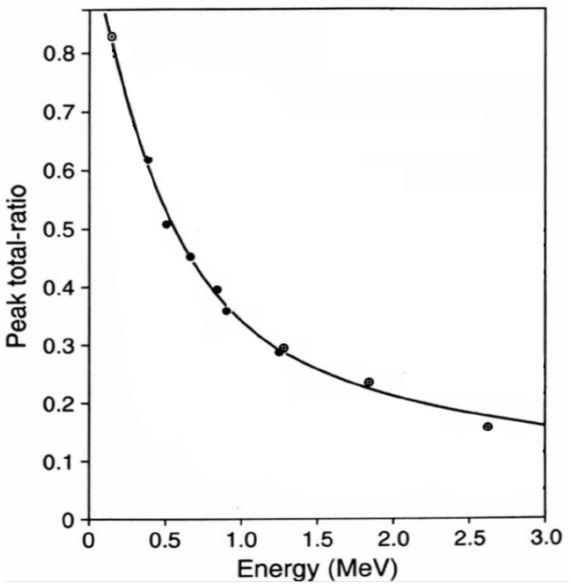

Figure 1: This plot shows the expected value for the peak to total. This plot can be understood by recognizing that the peak corresponding to the scattering photon shifts with different angles. As the scattering peak shifts towards the left, away from the incident peak, the peak to total ratio decreases. Please see Figures 8 and 9.

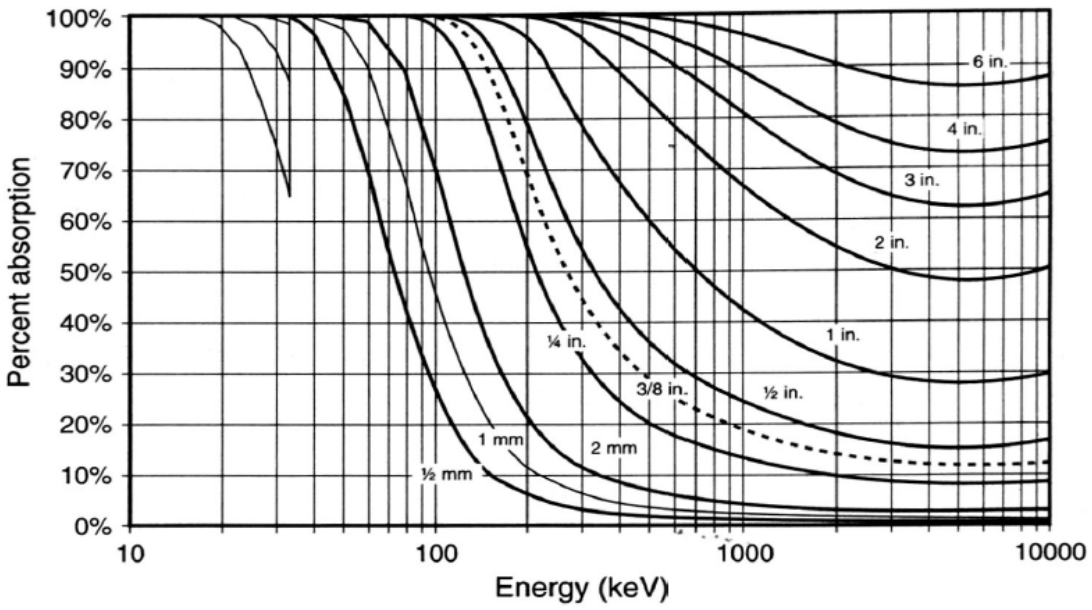

Figure 2: This figure shows the QE of several different NaI crystals. In this experiment, and the one done in Melissinos, the 3 inch crystal is used. It is readily seen that in the 100 to 1000 keV range, the QE of the 3 inch crystal is expected to be above 85 %. This image was taken from the URL in the Appendix.

Setting up the Experiment:

Figure 3 below shows the setup of the experiment.

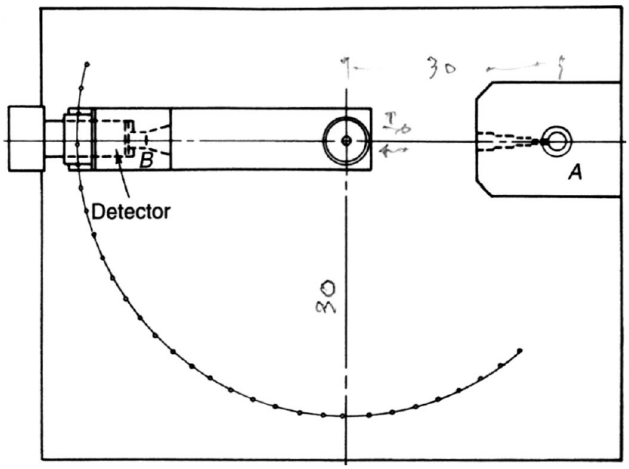

Figure 3: Physical setup of the experiment. The detector (B) is swung around the target and the bremsstrahlung continuum and emission spectra from the source (A) are measured at various angles.

Figure 4 below shows the block diagram of the circuit elements.

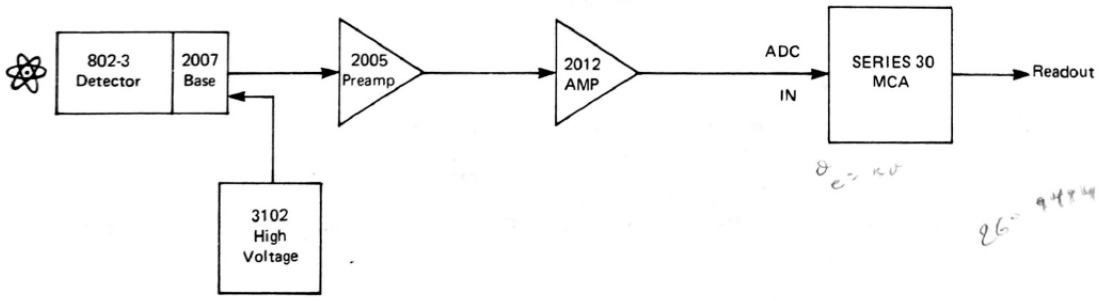

Figure 4: The block diagram of circuit elements shows how the detector converts the scintillation into an electrical pulse which then enters the MCA.

The Experiment:

Before the fun begins, a spectra is taken in order to do a two-point calibration, which requires two known energies. The first will be the source energy of ^{137}Cs (661 keV); in order to get a second known energy, a transparent element is placed in front of the source so that one of its emission lines can be picked up by the detector and used as the second known energy. ^{133}Ba (356 keV) is used for the second energy.

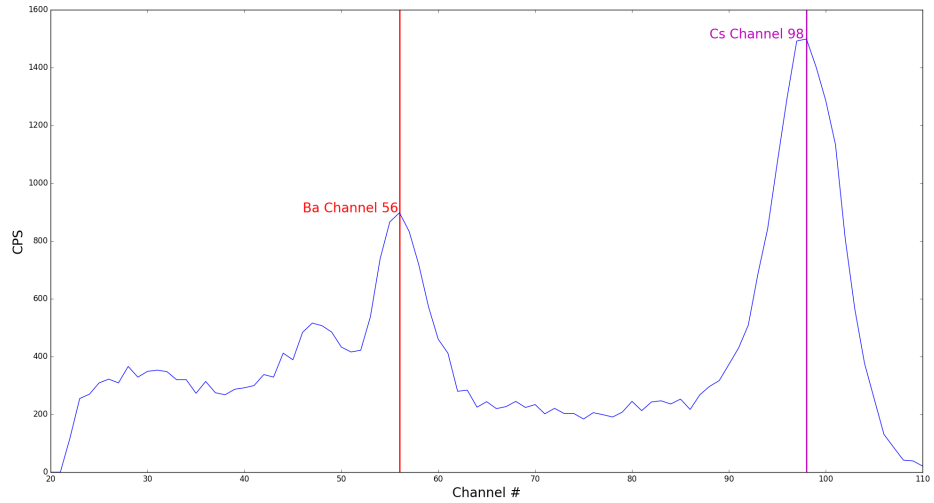

Figure 5: shows the spectra used for calibration. The red line at channel 56 corresponds with ^{133}Ba, while the magenta line at channel 98 corresponds with ^{137}Cs. See Table 1 in the below for more information on calibration.

Table 1: Calibration

	Channel #	keV
^{133}Ba	56	356
^{137}Cs	98	661

Coefficient	
A	-50.67
B	7.262

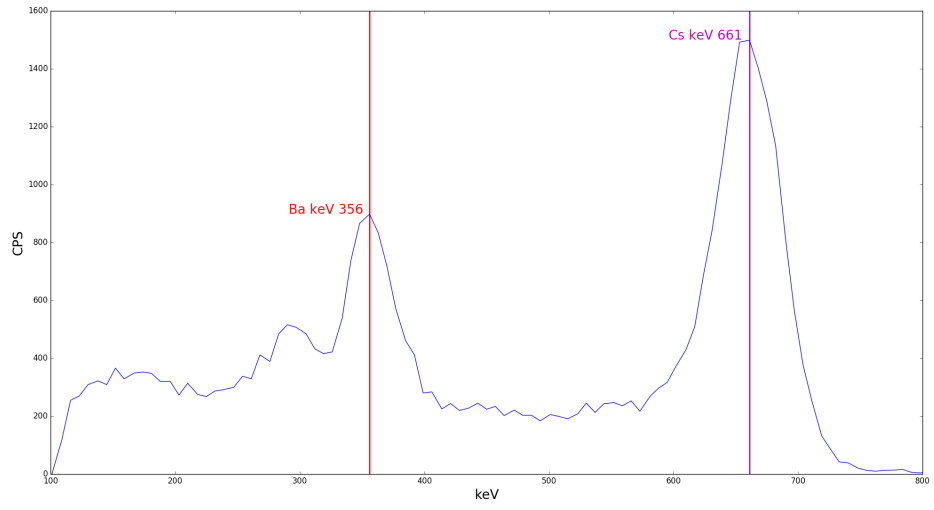

Figure 6: shows the calibration spectra after the the x-axis has been converted from channel space, to keV space. See Table 1 above for more information on calibration.

After the calibration is completed, two spectra are recorded for each 10 degree interval between 20 degrees

and 90 degrees; one is with the aluminium target and one is without. The reason for these contrasting spectra is so that scattering spectra and non scattering spectra can be compared. This comparison is shown below in Figure 7.

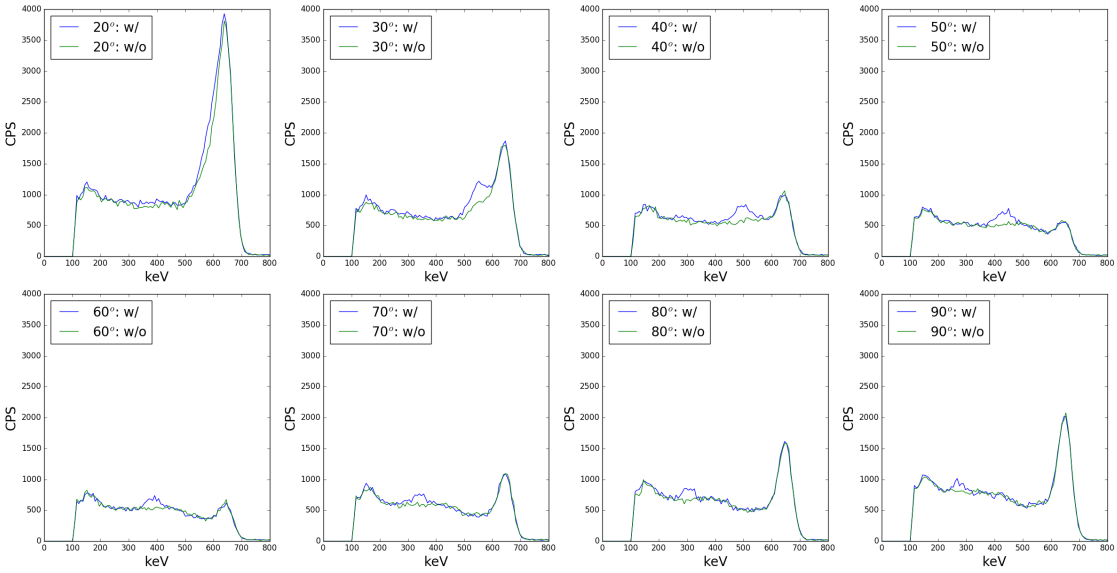

Figure 7: shows the spectra with (blue) and without (green) the target. The continuum depicted is Bremsstrahlung radiation with emission peaks.

In Figure 7 it is fairly easy to see the two emission peaks start to diverge around 30 degrees as the scattering energy shifts to the left with increasing scattering angle. In order to isolate the scattering spectra, the "with target" spectra must be subtracted from the "without target" spectra. This is shown below in Figure 8.

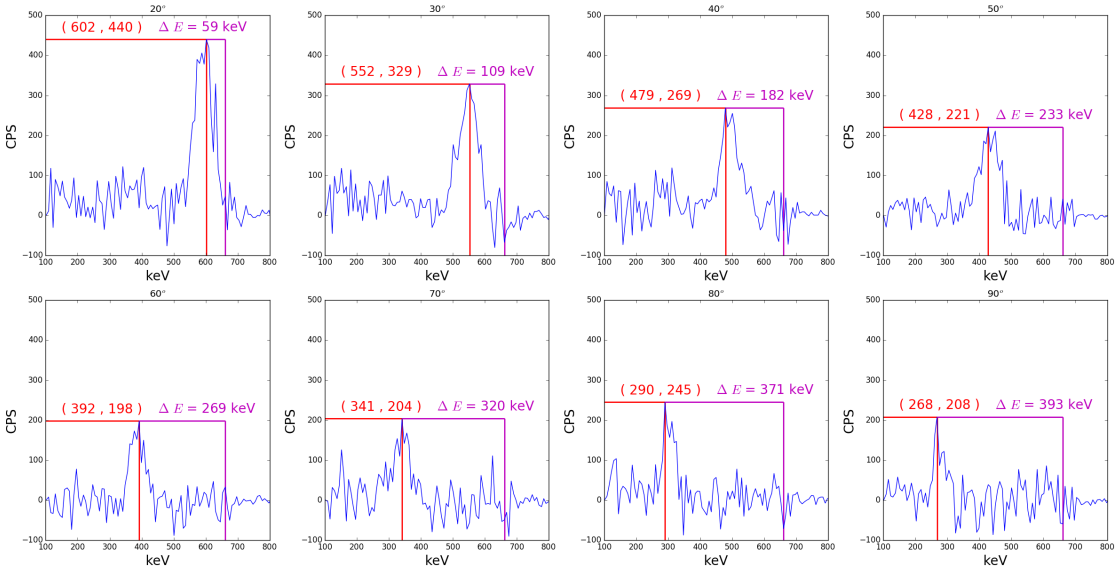

Figure 8: shows the spectra that result from subtracting the "with" and "without" spectra seen in Figure 7. The red vertical line indicates the apparent peak scattering energy and its position is annotated in red. The magenta vertical line indicates the un-scattered Energy of ^{137}Cs; the difference between the scattered and un-scattered energies are annotated in magenta.

After the scattering spectra is isolated, the peak is fit to a Gaussian curve. This is first accomplished by plotting a red Gaussian with the spectra max as the height, the center as the corresponding energy associated with the max height, and a standard deviation of 30. These are just the "guessing parameters entered into a Gaussian curve fitting algorithm in Python. This would then be used to find the peak to total ratios, but this model simply uses the tabulated data in Melissino's experiment instead. The results from the Gaussian fits are shown below in Figure 9.

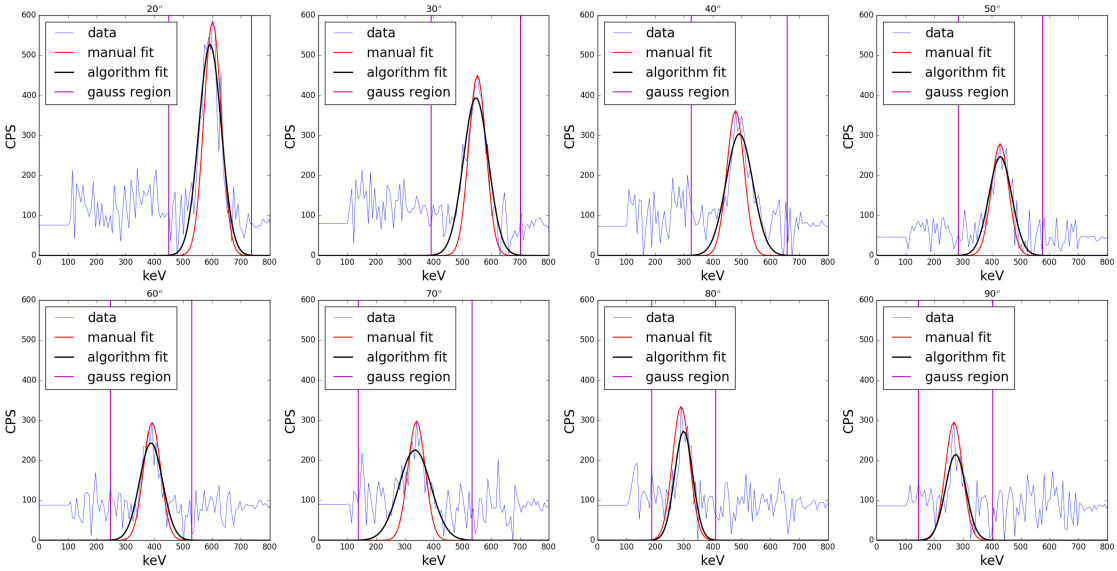

Figure 9: Each of the subtracted spectra are raised up so that the minimum spectra value is 0. The width is determined by finding the first value (coming from the left) where the Gaussian curve is greater than .1% of the peak value and subtracting it from the fitted average. The two magenta vertical lines represent the fitted average ± the found width. The region bounded by the two magenta lines is taken to be the scattered peak region.

Using the fitted peak energies and the scattering angle, Equation 1 is plotted using the data. A straight line is fit to the data which is used to determine electron rest mass, the results of which are shown below in Figure 10.

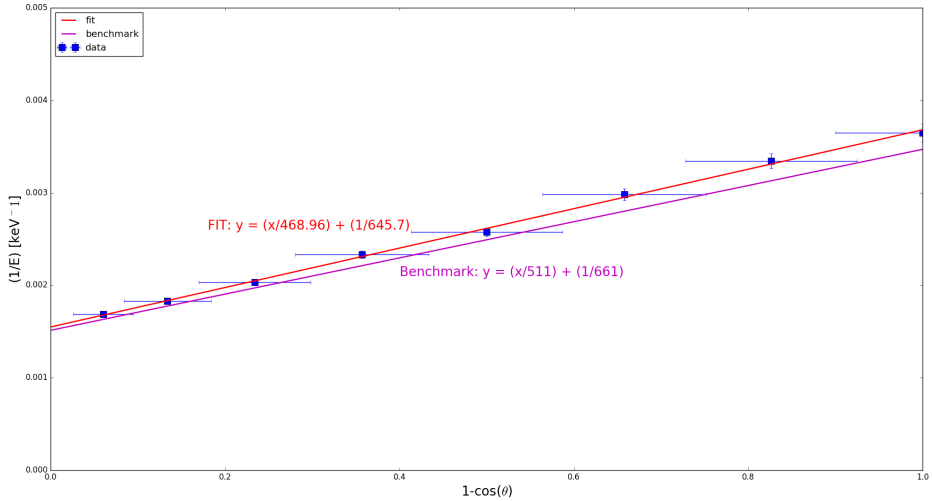

Figure 10: shows $1/E$ vs $1-\cos\theta$. Looking at the result of Equation 1, it is easy to see how this should form a line with $\frac{1}{m_e c^2}$ as the slope. The fitted line is shown in red, along with the equation found by fitting the data to a least squares algorithm in Python. A benchmark model using the known values for the electron rest energy and ^{137}Cs is also shown in magenta and is compared with the fitted line to justify the results. More information on the Compton fits can be found in Table 2 below.

Table 2: Compton Fits

	Fit	Benchmark	Err	% Err
$m_e c^2$ keV	468.96	551	42.040	8.2271
E keV	645.71	661	15.296	2.3141

The differential cross section is now constructed using Equations 8 and 9.

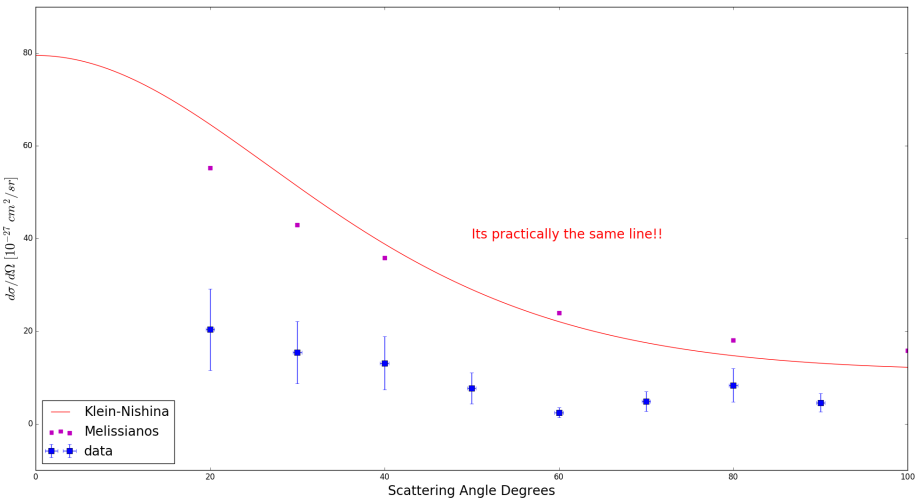

Figure 11: The data (blue squares) are compared with Melissinos data (magenta squares) and the Klein-Nishina theoretical line (red curve).

The results seen above seem to loosely agree with the Klein-Nishina and Mellisinos. There seems to be an unexplained secondary peak in the data as well. As of now, this secondary peak is assumed to be caused by some internal reflection in the experiment; additional followup experiments would have to confirm or falsify this assumption.

Table 3: Differential Cross Sections

Angle (^{o})	E' (keV)	Peak : Total	QE	$d\sigma/d\Omega$ $(1 \times 10^{-27} cm^2/sr)$	$\delta \frac{d\sigma}{d\Omega} \times 10^{-27} cm^2$
20	602	.47	.865	20.34	8.836
30	552	.50	.890	15.39	6.689
40	479	.53	.930	13.12	5.700
50	428	.55	.950	7.697	3.345
60	392	.57	.960	2.433	1.058
70	341	.61	.980	4.828	2.098
80	290	.65	.990	8.342	3.625
90	268	.69	.995	4.583	1.992

Discussion:

There seems to be a substantial margin for error in these results. Most of this error is not accounted for.

An easy source of error is found in the scattering angle recorded. The detector is moved by hand around

the target. The uncertainty in this measurement, $\Delta\theta$, is assumed to be .1 degrees.

The error shown along the x-axis in Figure 10 is calculated by Equation 10 below.

$$\begin{aligned} \delta x &= \frac{d}{d\theta}\Big(1-\cos\theta\Big)\Delta\theta \\ &= .1^o \sin\theta \end{aligned} \tag{10}$$

The error in the x-axis for Figure 11 is just $.1^o$ and is not noticeable on the plot.

Another source of error is found in converting the energy from the channel number. The error in finding the peak channel, Δx, is taken to be 1. The uncertainty in energy is then found using Equation 11 below.

$$\begin{aligned} \delta E &= \frac{d}{dx}(A+Bx)\Delta x \\ &= B\Delta x \\ &= 7.262\ keV \end{aligned} \tag{11}$$

Equation 11 implies that error in the y-axis found in Figure 10 can be found by,

$$\begin{aligned} \delta y &= \frac{d}{dE}\left(\frac{1}{E}\right)\Delta E \\ &= |\frac{-\Delta E}{E^2}| \\ &= \frac{7.262}{E^2}\ keV^{-1} \end{aligned} \tag{12}$$

The error from Equations 10 and 12 imply that the uncertainty in the electron rest mass found is found by,

$$\begin{aligned} \delta m_e c^2 &= \sqrt{\left[\frac{d}{dx}(m_e c^2)\Delta x\right]^2 + \left[\frac{d}{dy}(m_e c^2)\Delta y\right]^2} \\ m_e c^2 &= \left(\frac{1}{E'} - \frac{1}{E}\right)^{-1}(1-\cos\theta) \\ &= \left(y - \frac{1}{E}\right)^{-1} x \\ \Rightarrow \delta m_e c^2 &= \sqrt{\left[(y-\frac{1}{E})^{-1}\Delta x\right]^2 + \left[\frac{E^2 x \Delta y}{(Ey-1)^2}\right]^2} \\ \Rightarrow &= 105.80\ keV \end{aligned} \tag{13}$$

Since δy is energy dependant, Equation 13 will result in an array. This array is averaged to find a total uncertainty of 105.80 keV.

Now, for the differential cross section. This is found by,

$$
\begin{aligned}
\delta\frac{d\sigma}{d\Omega} &= \sqrt{(one)^2 + (two)^2 + (three)^2 + (four)^2} \\
(one) &= \frac{d}{d\text{yield}}\frac{d\sigma}{d\Omega}\Delta E \\
&= \frac{\Delta E}{d\Omega_d N_e I_{inc}} \\
(two) &= \frac{\text{yield}}{N_e I_{inc} d\Omega_d^2}\left(\frac{d}{d\Omega_d}\frac{d\sigma}{d\Omega}\Delta d_d \Delta r_d\right) \\
&= \frac{\text{yield}}{N_e I_{inc} d\Omega_d^2}\left(\frac{\pi d_d \Delta d_d}{2r_d^2} + \frac{\pi d_d^2 \Delta r_d}{2r_d^3}\right) \\
(three) &= \frac{\text{yield}}{d\Omega_d I_{inc} N_e^2}\left(\frac{d}{N_e}\frac{d\sigma}{d\Omega}\Delta h_t \Delta r_t\right) \\
&= \frac{\text{yield}}{d\Omega_d I_{inc} N_e^2}\left(\frac{2N_e \Delta r_t}{r_t} + \frac{N_e \Delta h_t}{h_t}\right) \\
(four) &= \Delta x
\end{aligned}
\tag{14}
$$

It turns out that $\delta\frac{d\sigma}{d\Omega}$ is also an array, which is why Figure 11 has varying y-error bars. The average of this error is found to be $4.1667 \times 10^{-27} cm^2$.

A full table of error related variables, their associated error, and their application can be found in Table 4 below.

Table 4: Error

Variable	Value	Uncertainty	Application
ΔE		7.262 keV	
δy		$\frac{\Delta E}{E^2}$	Compton Fit
$\Delta\theta$		0.1^o	Compton Fit
δx		$\Delta\theta \sin\theta$	Compton Fit
$\delta m_e c^2$		105.80 keV	Compton Fit
d_d	4.445 cm	0.127 cm	diameter of detector
r_{dt}	35.56 cm	0.127 cm	target to detector distance
d_t	3.3556 cm	0.127 cm	diameter of target
h_t	1.9 cm	0.127 cm	height of target
$\delta\frac{d\sigma}{d\Omega}$		$4.1678 \times 10^{-27} cm^2$	differential cross section

Appendix:

<http://www.crystals.saint-gobain.com/sites/imdf.crystals.com/files/documents/efficiency_calculations_brochure_69670.pdf>